Biomedicine & Pharmacotherapy 147 (2022) 112623

Contents lists available at ScienceDirect

Biomedicine & Pharmacotherapy

journal homepage: www.elsevier.com/locate/biopha

# Metabolomic changes after DAAs therapy are related to the improvement of cirrhosis and inflammation in HIV/HCV-coinfected patients

Ana Virseda-Berdices [a,b], David Rojo [c], Isidoro Martínez [a,b], Juan Berenguer [b,d,e], Juan González-García [b,f,g], Oscar Brochado-Kith [a,b], Amanda Fernández-Rodríguez [a,b], Cristina Díez [b,d,e], Víctor Hontañon [b,f,g], Leire Pérez-Latorre [b,d,e], Rafael Micán [b,f,g], Coral Barbas [c], Salvador Resino [a,b,*,1], María Angeles Jiménez-Sousa [a,b,*,1], on behalf of the ESCORIAL Study Group

[a] Unidad de Infección Viral e Inmunidad, Centro Nacional de Microbiología (CNM), Instituto de Salud Carlos III (ISCIII), Majadahonda, Madrid, Spain
[b] Centro de Investigación Biomédica en Red de Enfermedades Infecciosas, Instituto de Salud Carlos III, Madrid, Spain
[c] Centro de Metabolómica y Bioanálisis (CEMBIO), Departamento de Química y Bioquímica, Facultad de Farmacia, Universidad CEU-San Pablo, Urbanización Montepríncipe, 28925 Alcorcón, Madrid, Spain
[d] Unidad de Enfermedades Infecciosas/VIH; Hospital General Universitario "Gregorio Marañón", Madrid, Spain
[e] Instituto de Investigación Sanitaria Gregorio Marañón (IiSGM), Madrid, Spain
[f] Servicio de Medicina Interna-Unidad de VIH, Hospital Universitario La Paz, Madrid, Spain
[g] Instituto de Investigación Sanitaria La Paz (IdiPAZ), Madrid, Spain

ARTICLE INFO

*Keywords:*
Chronic hepatitis C
HIV
Cirrhosis
Metabolomics
DAAs therapy
HCV elimination

ABSTRACT

*Background:* A better understanding of the evolution of cirrhosis after hepatitis C virus (HCV) clearance is essential since the reversal of liver injury may not happen. We aimed to assess the evolution of plasma metabolites after direct-acting antivirals (DAAs) therapy and their association with liver disease scores in HIV/HCV-coinfected patients with advanced HCV-related cirrhosis.

*Methods:* We performed a prospective study in 49 cirrhotic patients who started DAAs therapy. Data and samples were collected at baseline and 36 weeks after SVR. Metabolomics analysis was carried out using gas chromatography-mass spectrometry and liquid chromatography-mass spectrometry. Inflammation-related biomarkers were analyzed using ProcartaPlex Immunoassays.

*Results:* At 36 weeks after SVR, patients experienced significant decrease in taurocholic acid, 2,3-butanediol, and LPC(18:0); while several phosphatidylcholines (LPC(16:1), LPC(18:1), LPC(20:4), and PC(16:0/9:0(CHO))/PC (16:0/9:0(COH)), 2-keto-n-caproic acid/2-keto-isocaproic acid and N-methyl alanine increased, compared to baseline. The plasma decrease in taurocholic acid was associated with a reduction in Child-Turcotte-Pugh (CTP) (AMR=3.39; q-value=0.006) and liver stiffness measurement (LSM) (AMR=1.06; q-value<0.001), the plasma

*Abbreviations:* HIV, Human immunodeficiency virus; HCV, Hepatitis C virus; DAAs, Direct-acting antivirals; LPC, Lysophosphatidylcholine; CTP, Child-Turcotte-Pugh score; AMR, Arithmetic mean ratio; LSM, Liver stiffness measurement; SVR, Sustained virological response; PCR, Polymerase chain reaction; cART, Combination antiretroviral therapy; INR, International normalized ratio; GC-MS, Gas chromatography–mass spectrometry; LC-MS, Liquid chromatography–mass spectrometry; QC, Quality control; MSD, Mass selective detector; ESI, Electrospray ionization; PLS-DA, Partial least squares discriminant analysis; LOOCV, Leave-one-out cross-validation; VIP, Variable importance in projection; GLMM, Generalized linear mixed-effects model; MELD, Model for End-stage Liver Disease; FDR, False discovery rate; PC, Phosphatidylcholine; LPS, Lysophosphatidylserine; IL, Interleukin; sRANKL, Soluble receptor activator of nuclear factor kappa-B ligand; OPG, Osteoprotegerin; PD, Programmed cell death protein; siCAM, Soluble intercellular adhesion molecule; IFN, Interferon; svCAM, Soluble vascular cell adhesion molecule; PAI, Plasminogen activator inhibitor; TNFRI, Tumor necrosis factor receptor 1; OxPL, Oxidized phospholipid; BCAA, Branched-chain amino acids; LPE, Lysophosphatidyletanolamine.

* Corresponding authors at: Unidad de Infección Viral e Inmunidad, Centro Nacional de Microbiología (CNM), Instituto de Salud Carlos III (ISCIII), Majadahonda, Madrid, Spain

*E-mail addresses:* virseda.ana@gmail.com (A. Virseda-Berdices), davidrb87@gmail.com (D. Rojo), imago@isciii.es (I. Martínez), jbb4@me.com (J. Berenguer), juangonzalezgar@gmail.com (J. González-García), brochado1993@gmail.com (O. Brochado-Kith), amandafr@isciii.es (A. Fernández-Rodríguez), crispu82@gmail.com (C. Díez), victor.hontanon@gmail.com (V. Hontañon), legor78@hotmail.com (L. Pérez-Latorre), micanrafael@hotmail.com (R. Micán), cbarbas@ceu.es (C. Barbas), sresino@isciii.es (S. Resino), jimenezsousa@isciii.es (M.A. Jiménez-Sousa).

[1] Both authors contributed equally to this study.

https://doi.org/10.1016/j.biopha.2022.112623
Received 14 December 2021; Received in revised form 5 January 2022; Accepted 5 January 2022
Available online 12 January 2022

increase in LPC(20:4) was related to a reduction in LSM (AMR=0.98; q-value=0.027), and the rise of plasma 2-keto-n-caproic acid/2-keto-isocaproic acid was associated with a reduction in CTP (AMR=0.35; q-value=0.004). Finally, plasma changes in taurocholic acid were directly associated with inflammation-related biomarkers, while changes in LPC(20:4) were inversely associated.

*Conclusions:* Plasma metabolomic profile changed after HCV clearance with all oral-DAAs in HIV/HCV-coinfected with advanced HCV-related cirrhosis. Changes in plasma levels of LPC (20: 4), 2-keto-n-caproic acid/2-keto-isocaproic acid, and taurocholic acid were related to improvements in cirrhosis scores and inflammatory status of patients.

## 1. Background

Hepatitis C virus (HCV) infection is one of the leading causes of chronic liver disease, cirrhosis, and hepatocellular carcinoma [1]. Furthermore, HCV infection is present in approximately 10–30% of HIV-infected patients, who have faster progression of cirrhosis, decompensation, or even death [2,3].

Newer direct-acting antivirals (DAAs) have revolutionized the prospects for HCV therapy by achieving success rates greater than 95% with minimal adverse events, improving the quality of life, and reducing cirrhosis-related morbidity [4]. Additionally, successful DAAs therapy in cirrhotic patients reduces the risk of liver complications and death [5]. Several non-invasive markers of liver fibrosis, based on imaging elastography or serum markers [6–8], also improve after the sustained virologic response (SVR) with DAAs therapy in patients with HCV-related cirrhosis [9–18]. However, it has been described that a subgroup of patients remains at risk of liver disease progression and hepatocellular carcinoma development [19]. Likewise, the persistence of portal hypertension in patients is frequent despite successful antiviral therapy, indicating a persistent risk of clinical progression or death [20].

Both HCV and HIV infection, as well as advanced liver cirrhosis, cause substantial metabolic alterations. Recently, it has been described that metabolic processes such as biosynthesis of fatty acids and phospholipids, cellular energy, oxidative stress, microbial metabolism, bile acids, insulin metabolism, and amino acid accumulation are altered in HIV/HCV-coinfected and HCV-monoinfected cirrhotic patients [21]. Besides, a set of lipid metabolites that allow earlier identification of HIV/HCV-coinfected patients at risk of developing clinically significant end-stage liver disease events has been recently described [22]. However, to our knowledge, there are no previous studies on the changes in the metabolomic profile after DAA therapy and its relationship with liver disease. A better understanding of the pathophysiology of cirrhosis after HCV clearance is essential for patient management.

This study aimed to evaluate the evolution of plasma metabolites after DAAs therapy and their association with liver disease scores in HIV/HCV-coinfected patients with advanced HCV-related cirrhosis.

## 2. Methods

### 2.1. Study subjects

We performed a multicenter longitudinal study in 49 HIV/HCV coinfected patients with advanced HCV-related cirrhosis who started DAAs therapy (without interferon (IFN) from January 2015 to June 2016 at four hospitals in Madrid, Spain (ESCORIAL study; see **Appendix**). This study was approved by the Research Ethics Committee of the Institute of Health Carlos III (CEI42_2020/CEI41_2014) and was carried out according to the Declaration of Helsinki. All participants gave their written informed consent before enrollment.

The inclusion criteria were: 1) baseline HCV infection confirmed by polymerase chain reaction (PCR); 2) advanced cirrhosis (liver stiffness ≥25 kPa, CTP ≥7, or hepatic liver pressure gradient (HVPG) ≥ 10 mmHg, or prior history of liver decompensation (ascites, bleeding esophageal varices, hepatic encephalopathy)); 3) starting anti-HCV therapy with all-oral DAAs and achieving an SVR (undetectable HCV-RNA load 12 weeks after the finalization of anti-HCV treatment); 4) stable combination antiretroviral therapy (cART) ≥ 6 months and undetectable plasma HIV viral load (<50 copies/mL). 5) Available samples of frozen plasma at the start of HCV treatment (baseline) and 36 weeks after SVR (end of follow-up).

### 2.2. Clinical data and samples

Epidemiological and clinical data were prospectively collected, using an online form that met the confidentiality requirements, and monitored to verify its accordance with the patient's medical records. Child-Turcotte-Pugh (CTP) score was calculated based on the following factors: total bilirubin, serum albumin, international normalized ratio (INR), ascites, and hepatic encephalopathy. CTP score can range from 5 to 15 points. As previously described, trained operators carried out the transient elastography to obtain the liver stiffness measurement (LSM) [23].

Peripheral blood samples were collected in EDTA tubes. Plasma samples were separated by centrifugation and stored at − 80ºC in the Spanish HIV HGM Biobank until use.

### 2.3. Non-targeted metabolomics

#### 2.3.1. Reagents and standards for metabolomics

The list of reagents and standards is available in Supplemental Data 1.

#### 2.3.2. Metabolite extraction and sample preparation

Firstly, viruses in samples were inactivated by mixing plasma with methanol (3:1, v/v). Then, plasma samples were vortexed for 15 seg, kept cold for 5 min, centrifuged at 16,000 g, 4 ºC for 20 min, and stored at − 80 ºC until they were sent to the Center for Metabolomics and Bioanalysis (San Pablo-CEU University, Madrid, Spain).

The samples were processed for their subsequent measurement on the analysis day by gas chromatography-mass spectrometry (GC-MS) and liquid chromatography-mass spectrometry (LC-MS). Quality controls (QCs) samples were prepared independently for each analytical platform by pooling and mixing equal volumes of each corresponding sample (full description in Supplemental Data 1).

#### 2.3.3. Data acquisition

According to a methodology previously used, the metabolomic analysis was performed using two complementary analytical platforms [24]. A GC system (Agilent Technologies 7890 A) was used consisting of an autosampler (Agilent Technologies 7693) and an inert mass selective detector (MSD) with quadrupole (Agilent Technologies 5975). The derivatized samples were injected through a GC-Column DB5-MS (30 m length, 0.25 mm internal diameter, 0.25 μm film 95% dimethylpolysiloxane / 5% diphenyl-polysiloxane) with a pre-column (10 m J&W integrated with Agilent 122–5532G). An LC system consisting of a degasser, a binary pump, and an autosampler (1290 infinity II, Agilent) was also used to increase the metabolite coverage. The samples were injected into a reversed-phase column (Zorbax Extend C18 50 × 2.1 mm, 1.8 μm; Agilent). The mobile phases were solvent A ($H_2O$ containing 0.1% formic acid) and solvent B (acetonitrile containing 0.1% formic

acid). Data were collected in positive and negative electrospray ionization (ESI) modes in separate runs using Q-TOF (Agilent 6550 iFunnel) (full description in Supplemental Data 1).

#### 2.3.4. Data treatment and quality assurance

In GC-MS, the deconvolution and identification were performed using MassHunter Quantitative Unknowns Analysis (B.07.00, Agilent), alignment with MassProfiler Professional software (version 13.0, Agilent), and peak integration using MassHunter Quantitative Analysis (version B.07.00, Agilent). In LC-MS, the Molecular Feature Extraction and the Recursive Feature Extraction algorithms in the MassHunter Profinder software (B.08.00, Agilent) were used for deconvolution and alignment of the raw data. After data reprocessing, the metabolic features were filtered (quality assurance details are available in Supplemental Data 1).

### 2.4. Inflammatory markers

ProcartaPlex multiplex immunoassay (Bender MedSystems GmbH, Vienna, Austria) was used to measure the plasma concentrations of D-Dimer, IFN-γ, IL10, IL12p70, IL17A, IL18, IL1-β, IL1RA, IL2, IL4, IL6, IL8, Insulin, IP10, Leptin, MCP1, OPG, PAI1, PD1, PDL1, sICAM1, sRANKL, sVCAM1, TGF-β, TNF-α, TNFRI, VEGF-α and VEGFR1 (Supplemental Data 2). The manufacturer's specifications were followed using a Luminex 200™ analyzer (Luminex Corporation, Austin, TX, United States).

### 2.5. Statistical analysis

The statistical analysis was performed using MetaboAnalyst 4.0 software (http://www.metaboanalyst.ca/) and R statistical package (R Foundation for Statistical Computing, Vienna, Austria).

For the multivariate analysis, firstly, variables from GC-MS and LC-MS were log-transformed ($log_2$) and auto-scaled. Next, we performed a supervised multivariate analysis by partial least squares discriminant analysis (PLS-DA), which models all features together. Cross-validation with leave-one-out cross-validation (LOOCV) obtaining $R^2$ and $Q^2$ values as performance measures were performed. Variable importance in projection (VIP) score for each feature was obtained from the PLS-DA model. A permutation test was used to confirm the model's validity by separation distance (B/W) with a permutation number set at 1000. A $p < 0.05$ in the permutation test was considered significant to confirm the validity of the PLS-DA models.

Differences between plasma feature levels in paired groups were analyzed by Wilcoxon tests. For the association analysis, we used Generalized Linear Mixed-effects Model (GLMM) with gamma distribution ($log_2$-transformed values with identity-link for variables from LC-MS and raw values with log-link for variables from GC-MS; 'glm function' in R) to study the changes of features (dependent variable) from baseline to 36 weeks after SVR (independent variable). This test provides the arithmetic means (AMR) ratio and the significance level. Additionally, we performed GLMM with gamma distribution to study the association between plasma features (dependent variable) with liver disease markers (CTP and LSM, as independent variables).

For those features significantly associated with some liver disease markers, their relationship with inflammatory biomarkers was also analyzed using GLMM. In all cases, p-values were corrected for multiple testing by the false discovery rate (*FDR*) with Benjamini and Hochberg procedure ('qvalue package' in R).

### 2.6. Metabolite identification

The significant features were identified based on FiehnLib [25], NIST 14 libraries, and the CEU Mass Mediator search tool (http://ceumass.eps.uspceu.es) [26]. The metabolites were reported in agreement with the criteria of the Metabolomics Standards Initiative [27,28]. Further details are available in Supplemental Data 1.

## 3. Results

### 3.1. Patient characteristics

Clinical and epidemiological characteristics of 49 HIV/HCV-coinfected patients are shown in Table 1. The median age was 52 years, 77.6% were male, 10.2% reported a high current alcohol intake, 75.5% were IVDU, 34.7% had prior AIDS diagnosis, and 46.9% had previously failed anti-HCV IFN antiviral therapy.

### 3.2. Changes in plasma metabolites from baseline to 36 weeks after SVR

PLS-DA analysis was performed for features detected in GC-MS, LC-MS ESI(+), and LC-MS ESI(-) (Fig. 1**A**) and validated by permutation ($p < 0.001$) (Fig. 1**B**). The PLS-DA score graphs showed the two sets of samples, baseline and final (36 weeks after SVR), clearly separated. A

**Table 1**
Clinical and epidemiological characteristics of HIV-HCV coinfected patients.

| | HIV-HCV coinfected patients |
|---|---|
| No. | 49 |
| Age (years) | 52 (49–54) |
| Gender (male) | 38 (77.6%) |
| BMI (kg/m$^2$) | 24.0 (22.0–25.5) |
| Smoker (n = 48) | |
| Never | 6 (12.5%) |
| Previous (≥ 6 months) | 12 (25.0%) |
| Current | 30 (62.5%) |
| Alcohol intake (>50 g/day) | |
| Never | 21 (42.9%) |
| Previous (≥ 6 months) | 23 (46.9%) |
| Current | 5 (10.2%) |
| IVDU | 37 (75.5%) |
| Previous anti-HCV therapy | 23 (46.9%) |
| Treatment with statins | 8 (16.3%) |
| **Other liver markers** | |
| MELD | 9 (8–10) |
| LSM | 31.5 (22.0–39.3) |
| HVPG (n = 23) | 15.0(11.5–17.0) |
| Ascites | 14 (28.6%) |
| Bleeding esophageal varices | 20 (40.8%) |
| Hepatic encephalopathy | 5 (10.2%) |
| Carcinoma hepatocellular | 0 (0%) |
| **HCV markers** | |
| HCV genotype (n = 48) | |
| 1 | 32 (66.7%) |
| 2 | 0 (0%) |
| 3 | 6 (12.5%) |
| 4 | 10 (20.8%) |
| $Log_{10}$ HCV-RNA (IU/mL) (n = 89) | 6.2 (5.7–6.7) |
| HCV-RNA > 850,000 IU/mL | 32 (65.3%) |
| **HIV markers** | |
| Previous AIDS (n = 49) | 17 (34.7%) |
| Nadir CD4$^+$ T cells (n = 45) | 119 (70–182) |
| Nadir CD4$^+$ T cells< 200 cells/mm$^3$ (n = 45) | 34 (75.6%) |
| Baseline CD4$^+$ T cells (n = 49) | 444 (241–721) |
| Baseline CD4$^+$ T cells< 500 cells/mm$^3$ (n = 49) | 29 (59.2%) |
| **Antiretroviral therapy** (n = 48) | |
| NRTI+NNRTI | 7 (14.6%) |
| NRTI+II | 23 (47.9%) |
| NRTI+PI | 5 (10.4%) |
| PI+II+NNRTI/MVC | 4 (8.3%) |
| Others | 9 (18.8%) |

Values are expressed as absolute number (percentage) and median (interquartile range). Abbreviations: BMI, body mass index; IVDU, intravenous drug user; HCV, hepatitis C virus; HCV-RNA, HCV plasma viral load; HIV, human immunodeficiency; MELD, model for end-stage liver disease; LSM, liver stiffness measurement; AIDS, acquired immune deficiency syndrome; NNRTI, non-nucleoside analogue HIV reverse transcriptase inhibitor; NRTI, nucleoside analogue HIV reverse transcriptase inhibitor; PI, protease inhibitor; II, integrase inhibitor, MVC, maraviroc.

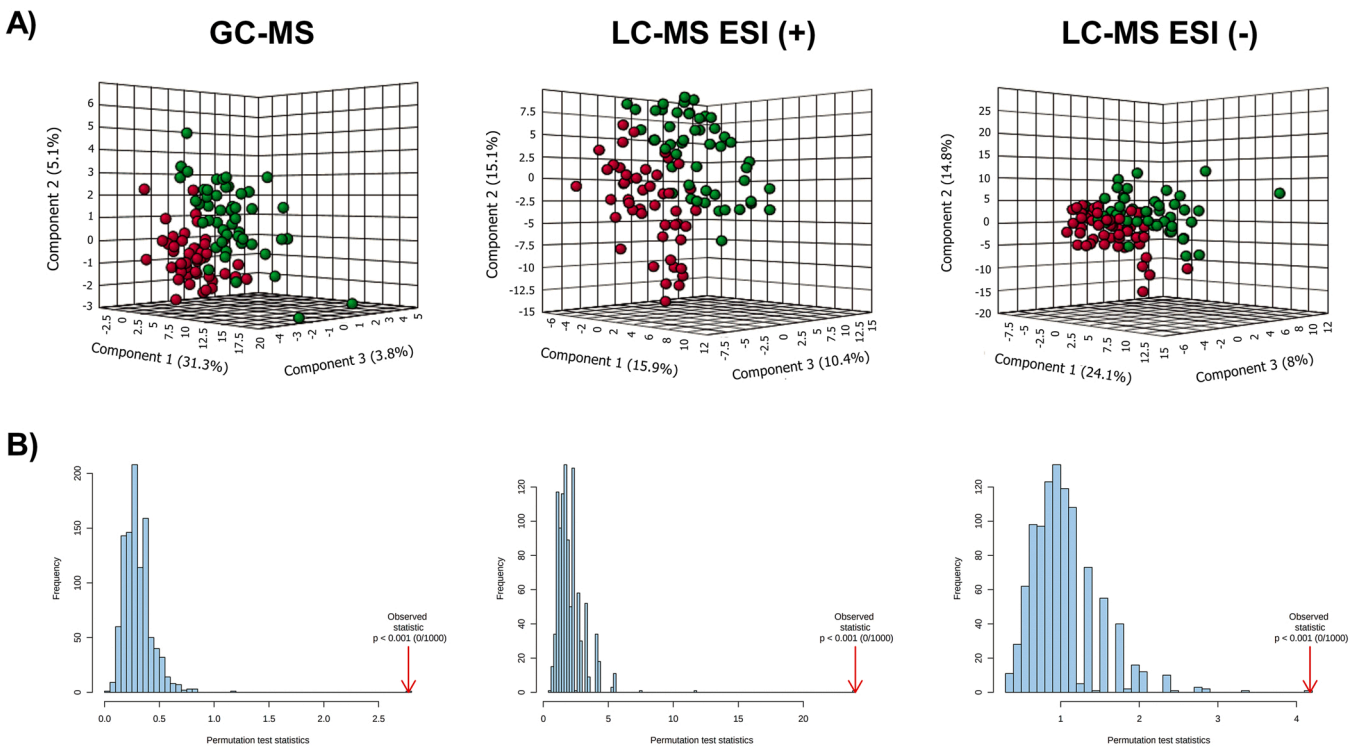


**Fig. 1.** Multivariate analysis of plasma metabolites comparing baseline (before DAA therapy; circles in green) and final (36 weeks after SVR; circles in red) time points in HIV/HCV-coinfected patients (n = 49). (A) partial least squares discriminant analysis (PLS-DA) plots resulting from GC-MS, LC-MS ESI(+), and LC-MS ESI(-) data. (B) Permutation by separation distance (B/W) with a permutation number of 1000 was used to confirm the validity of the PLS-DA models. $P < 0.001$ was obtained for GC-MS, LC-MS ESI+ and ESI-, validating the PLS-DA models. Abbreviations: GC-MS, gas chromatography-mass spectrometry; LC-MS, and liquid chromatography-mass spectrometry; ESI, electrospray ionization.

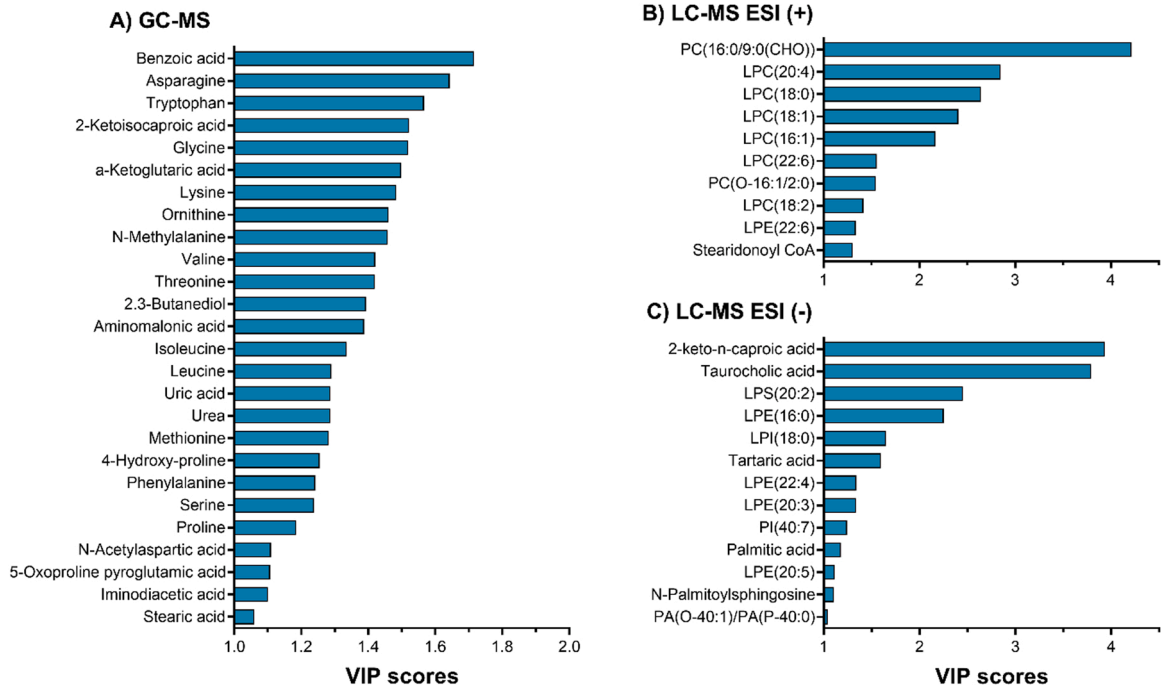


**Fig. 2.** Metabolites with the highest VIP score (≥1) in discriminating before and 36 weeks after SVR from PLS-DA models (n = 49). VIP score measures the variable's importance and allows metabolites to be ranked according to their importance. VIP≥ 1 was considered significant. Abbreviations: GC-MS, gas chromatography-mass spectrometry; LC-MS, and liquid chromatography-mass spectrometry; ESI, electrospray ionization; PC, phosphatidylcholine; LPC, lysophosphatidylcholine; LPE, lysophosphatidylethanolamine; LPS, lysophosphatidylserine; LPI, lysophosphatidylinositol; PA, phosphatidic acid; PC(16:0/9:0(CHO)), PC(16:0/9:0(CHO))/PC (16:0/9:0(COH)); 2-keto-n-caproic acid, 2-keto-n-caproic acid/2-keto-isocaproic acid.

VIP value for each detected feature was obtained from PLS-DA analysis. The VIP score is a quantitative estimation of the discriminatory power of each feature, allowing metabolites to be ranked according to their importance in discriminating the groups analyzed. Features with VIP≥ 1 were considered significant, but only 26 of 32 in GC-MS, 10 of 67 in LC-MS ESI (+), and 13 of 56 in LC-MS ESI (-) could be identified (Supplemental Data 3). The highest VIP scores were observed for PC(16:0/9:0(CHO))/PC(16:0/9:0(COH)), LPC(20:4), LPC(18:0), LPC(18:1) and LPC(16:1) in LC-MS ESI(+) (VIP= 4.22, 2.85, 2.64, 2.41, and 2.16, respectively) and 2-keto-n-caproic acid/2-keto-isocaproic acid, taurocholic acid, LPS(20:2) and LPE(16:0) in LC-MS ESI(-) (VIP= 3.94, 3.79, 2.45, and 2.25, respectively) (Fig. 2; full description in Supplemental Data 3).

By GLMM analysis, 28 significant features were found, of which nine features could be identified. At 36 weeks after SVR, patients experienced a significant increase in plasma levels of N-methylalanine (AMR(95% confidence interval (CI)= 2.85(1.72–4.74); q= 0.004), LPC (16:1) (AMR (95%CI)= 1.39(1.14–1.70); q= 0.022), LPC (18:1) (AMR(95%CI)= 1.34(1.13–1.59); q= 0.015), LPC (20:4) (AMR(95%CI)= 1.53 (1.26–1.86); q< 0.001), PC 16:0/9:0(CHO)/PC(16:0/9:0(COH)) (AMR (95%CI)= 1.50(1.33–1.69); q< 0.001), and 2-keto-n-caproic acid/2-keto-isocaproic acid (AMR(95%CI)= 2.32(1.41–3.82), q= 0.048), compared to baseline. However, 2,3-butanediol (AMR(95%CI)= 0.44 (0.27–0.67); q= 0.005), LPC (18:0) (AMR(95%CI)= 0.70(0.58–0.84); q= 0.004) and taurocholic acid (AMR(95%CI)= 0.29(0.18–0.45); q< 0.001) significantly decreased during follow-up (Table 2; Supplemental Data 4). These metabolites that remained significant after adjustment for multiple comparisons in the association analysis were consistent with those metabolites that had a higher VIP score in the multivariate analysis.

### 3.3. Association between changes in plasma metabolites and cirrhosis scores

We found a significant association of 25 and 35 metabolic features with CTP and LSM scores, respectively. Two metabolic features for each liver score had a q-value< 0.05 and could be identified. Increased plasma level of LPC(20:4) was associated with a decrease in LSM (AMR (95%CI)= 0.98(0.97–0.99); q-value= 0.027), increased plasma level of 2-keto-n-caproic acid/2-keto-isocaproic acid was related to the reduction of CTP score (AMR(95%CI)= 0.35(0.22–0.57) (1.87–6.14); q-value= 0.004), and decreased plasma level of taurocholic acid was associated with the reduction of CTP (AMR(95%CI)= 3.39; q-value= 0.006) and LSM (AMR(95%CI)= 1.06(1.04–1.09); q-value< 0.001) (Table 3).

**Table 2**
Changes in blood metabolome from baseline to 48 weeks after completion of DAA therapy.

| Metabolite | Technology | AMR (95%CI) | *p-value* | *q-value* |
|---|---|---|---|---|
| 2,3-Butanediol | GC-MS | 0.44 (0.27–0.67) | **< 0.001** | **0.005** |
| N-Methylalanine | GC-MS | 2.85 (1.72–4.74) | **< 0.001** | **0.004** |
| LPC(16:1) | LC-MS ESI + | 1.39 (1.14–1.70) | **0.001** | **0.022** |
| LPC(18:0) | LC-MS ESI + | 0.70 (0.58–0.84) | **< 0.001** | **0.004** |
| LPC(18:1) | LC-MS ESI + | 1.34 (1.13–1.59) | **< 0.001** | **0.015** |
| LPC(20:4) | LC-MS ESI + | 1.53 (1.26–1.86) | **< 0.001** | **< 0.001** |
| PC(16:0/9:0(CHO))* | LC-MS ESI + | 1.50 (1.33–1.69) | **< 0.001** | **< 0.001** |
| 2-keto-n-caproic acid* | LC-MS ESI - | 2.32 (1.41–3.82) | **< 0.001** | **0.048** |
| Taurocholic acid | LC-MS ESI - | 0.29 (0.18–0.45) | **< 0.001** | **< 0.001** |

Statistics: Associations were calculated by Generalized Linear Mixed-effects Model (GLMM) with a gamma distribution (identity-link to variables from LC-MS and log-link to variables from GC-MS); q-values represent p-values corrected for multiple testing using the False Discovery Rate (FDR). Significant differences are shown in bold. Abbreviations: AMR, arithmetic mean ratio; 95% CI, 95% of confidence interval; p-value, level of significance; q-value, corrected level of significance; HIV, Human immunodeficiency virus; HCV, Hepatitis C virus; LPC, lysophosphatidylcholine; PC, phosphatidylcholine; PC(16:0/9:0(CHO))*, PC(16:0/9:0(CHO))/PC(16:0/9:0(COH)); 2-keto-n-caproic acid*, 2-keto-n-caproic acid/2-keto-isocaproic acid.

### 3.4. Association between changes in cirrhosis-related metabolites and inflammation

The increase in LPC (20:4) was associated with a reduction in plasma levels of IL6, IL8, IL10, IL12p70, IL18, sRANKL, OPG, siCAM1, PD1, and IFN-γ (inverse association). The reduction in taurocholic acid was related to decreased levels of IL1RA, IL6, IL8, IL10, IL12p70, IL18, IP10, OPG, svCAM1, siCAM1, PAI1, and TNFRI (direct association) (Fig. 3; the full description in Supplemental Data 5). No significant results were found for 2-keto-n-caproic acid/2-keto-isocaproic acid.

## 4. Discussion

This study describes how metabolomics profile changes after SVR with DAAs therapy in HCV/HIV coinfected patients with advanced liver cirrhosis. A decreased taurocholic acid and increased LPC(20:4) and 2-keto-n-caproic acid/2-keto-isocaproic acid levels in plasma were associated with reductions in liver disease scores (CTP and LSM). Additionally, plasma levels of taurocholic acid and LPC(20:4) were related to the inflammatory state. To date, there is scarce information in the literature about metabolic changes after HCV eradication with DAAs. Only Meoni et al. [29] studied the metabolomic profile in HCV-monoinfected patients before and after successful viral eradication with DAAs therapy, describing several dysregulated pathways. However, to our knowledge, our study assesses for the first time the metabolomic changes after HCV eradication among HIV/HCV-coinfected patients.

In this study, several lysophosphatidylcholines such as LPC (16:1), LPC (18:1), and LPC (20:4) significantly increased at 36 weeks after SVR. Our results are consistent with an improvement in liver disease since reduced levels of plasma LPC have been described in advanced stages of HCV-related cirrhosis [21] and other inflammatory diseases, such as obesity [30], type 2 diabetes [31], and chronic ischemic stroke [32]. For LPC (20:4), this hypothesis was confirmed when we found the relationship between an increase in LPC (20:4) levels and an improvement in liver disease scores (CTP and LSM). This finding is also in accordance with previous studies, in which LPC (20:4) was downregulated in patients with hepatocellular carcinoma versus healthy volunteers [33]. Additionally, diminished levels of LPC were associated with inflammation status [34], which is in agreement with the inverse association found in our study between increased levels of LPC (20:4) after SVR and decreased levels of inflammation-related biomarkers (IL6, IL8, IFN-γ, IL12p70, IL18, IL-10, sICAM1, sRANKL, OPG, and PD-1). Therefore, increased LPC levels after SVR were linked to lower cirrhosis severity and inflammation.

We also observed that levels of an oxidized phospholipid (OxPL), PC (16:0/9:0(CHO))/PC(16:0/9:0(COH)), increased after SVR. Although OxPLs have been widely associated with oxidative stress, OxPLs have also demonstrated tissue-protective and anti-inflammatory activities, contributing to the resolution of inflammation [35,36]. Thus, the increase of this metabolite during follow-up could be involved in this protective effect. It has been described that OxPLs can exert anti-inflammatory activity by induction of drug metabolism phase II genes, leading to protection from oxidant stress [35]. However, further research would be needed to corroborate the effect of OxPL after DAAs therapy.

We also found that levels of 2-keto-n-caproic acid/2-keto-isocaproic acid increased at 36 weeks after SVR and were inversely correlated with the CTP score. This finding agrees with previous studies, which have shown that branched-chain amino acid (BCAA) supplementation was related to an improved prognosis of cirrhotic patients [37,38]. However, although leucine and other BCAAs have many positive repercussions on metabolism in multiple tissues, elevated levels of leucine and their metabolites, such as the keto-isocaproic acid, have also been associated

**Table 3**
Association between plasma metabolites and liver disease markers from baseline to 48 weeks after completion of DAA therapy.

| | | CTP score | | | LSM (kPa) | | |
|---|---|---|---|---|---|---|---|
| Metabolite | Technology | AMR (95%CI) | *p-value* | *q-value* | AMR (95%CI) | *p*-value | *q*-value |
| LPC(20:4) | LC-MS ESI+ | 0.69 (0.56–0.87) | **0.001** | 0.091 | 0.98 (0.97–0.99) | **< 0.001** | **0.027** |
| 2-keto-n-caproic acid* | LC-MS ESI- | 0.35 (0.22–0.57) | **< 0.001** | **0.004** | 0.99 (0.96–1.01) | 0.254 | 0.724 |
| Taurocholic acid | LC-MS ESI- | 3.39 (1.87–6.14) | **< 0.001** | **0.006** | 1.06 (1.04–1.09) | **< 0.001** | **< 0.001** |

Statistics: Associations were calculated by Generalized Linear Mixed-effects Model (GLMM) with a gamma distribution; q-values represent p-values corrected for multiple testing using the False Discovery Rate (FDR). Significant differences are shown in bold.
**Abbreviations:** AMR, the ratio of the arithmetic means; 95%CI, 95% of confidence interval; p, level of significance; q, corrected level of significance; CTP, Child-Turcotte-Pugh score; MELD, model of end-stage liver dysfunction; LSM, liver stiffness measure**;** LPC, lysophosphatidylcholine; 2-keto-n-caproic acid* : 2-keto-n-caproic acid/2-keto-isocaproic acid.

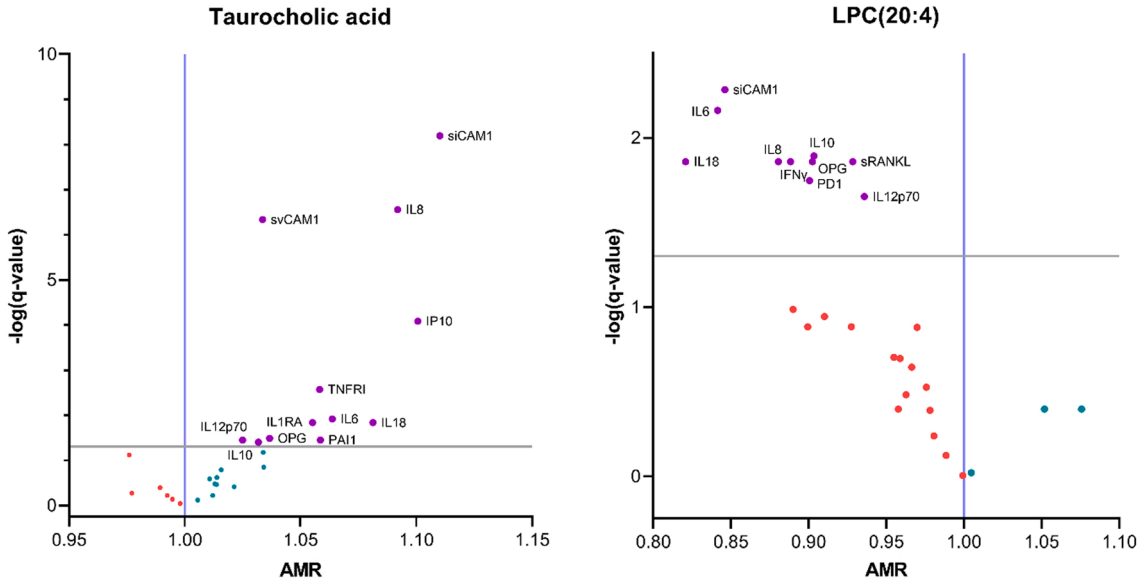


**Fig. 3.** Association between metabolites related to cirrhosis scores and inflammation-related biomarkers throughout the follow-up (from baseline to 36 weeks after SVR) (n = 49). Data were calculated by Generalized Linear Mixed-effects Model (GLMM), correcting for multiple testing by using the false discovery rate (FDR) with Benjamini and Hochberg procedure. Biomarkers that were associated with taurocholic acid: IL10 (p = 0.017; q=0.039), IL12p70 (p = 0.013; q=0.036), IL-18 (p = 0.004; q=0.015), IL1RA (p = 0.004; q=0.015), IL6 (p = 0.003; q=0.012), IL8 (p < 0.001; q<0.001), IP10 (p < 0.001; q<0.001), OPG (p = 0.010; q=0.033), PAI1 (p = 0.014; q=0.036), sICAM1 (p < 0.001; q<0.001), sVCAM1 (p < 0.001; q<0.001), TNFR1 (p < 0.001; q=0.003). Biomarkers that were associated with LPC (20:4): IFN gamma (p = 0.004; q=0.014), IL10 (p = 0.001; q=0.013), IL12p70 (p = 0.008; q=0.022), IL18 (p = 0.003; q=0.014), IL6 (p < 0.001; q=0.014), IL8 (p = 0.003; q=0.014), OPG (p = 0.003; q=0.014), PD1 (p = 0.006; q=0.018), sICAM1 (p < 0.001; q=0.005), sRANKL(p = 0.004; q=0.014). Abbreviations: q-value, p-value adjusted by for the false discovery rate (FDR); AMR, arithmetic mean ratio; LPC, lysophosphatidylcholine; IL, interleukin; sRANKL, soluble receptor activator of nuclear factor kappa-B ligand (also known as tumor necrosis factor ligand superfamily member 11 (TNFSF11)); OPG, osteoprotegerin (also known tumor necrosis factor receptor superfamily member 11b (TNFRSF11B)); svCAM1, soluble vascular cell adhesion molecule 1; siCAM1, soluble intercellular adhesion molecule-1; PD1; programmed cell death protein 1; IFN, interferon; IP10, C-X-C motif chemokine ligand 10 (also known as CXCL10); PAI1, plasminogen activator inhibitor type 1; TNFRI, tumor necrosis factor receptor 1.

with metabolic disturbances [39] and correlated positively with body fat percentage [40]. This particular finding could be related to the weight gain experienced in patients after HCV cure with DAA therapy [41]. In contrast, little information is available on the role of N-methylalanine in liver disease. In our study, we observed an increase in N-methylalanine levels after SVR. This metabolite has been described as a urine metabolite implicated in the development of hepatic encephalopathy [42]. However, further studies are needed for more specific information about its role in the evolution of liver disease among HIV/HCV-coinfected patients. Regarding 2,3-butanediol, a bacterial fermentation product, its increased level has been directly associated with advanced cirrhosis among HCV-infected patients with or without HIV infection in previous studies [21]. This metabolite has been linked to dynamic shifts in microbiota diversity [43]. Thus, the decrease in 2,3-butanediol observed in our study could be related to normalization changes in microbiome diversity and improved liver disease after DAA therapy.

Bile acids have been widely associated with the progression of liver cirrhosis, with taurocholic acid being the most increased metabolite in cirrhotic patients compared to healthy controls [44]. Besides, taurocholic acid has also been positively associated with CTP classification [21,44]. However, to our knowledge, no previous report has described its evolution after HCV elimination. In this regard, we found that levels of taurocholic acid decreased after SVR. Moreover, we observed that changes in taurocholic acid levels were directly associated with liver disease scores (CTP and LSM). It demonstrated that taurocholic acid decrease is related to an improvement in liver disease after SVR in HIV/HCV-coinfected patients. Additionally, we have also observed that the reduction in plasma levels of taurocholic acid after SVR is directly associated with a decrease in levels of inflammation-related biomarkers (IL1RA, IL6, IL8, IL10, IL12p70, IL18, TNFRI, IP10, svCAM1, siCAM1, OPG, and PAI1). Thus, taurocholic acid could be a crucial marker of liver disease, both of cirrhosis progression and remission after HCV elimination with DAA therapy.

In addition, many amino acids increased at 36 weeks after SVR, such as asparagine, tryptophan, glycine, lysine, ornithine, valine, threonine, isoleucine, leucine, methionine, phenylalanine, serine, and proline.

Amino acids are involved in various biological processes and have even been proposed as therapeutical agents in liver diseases [45]. Many of them can improve the immune response and decrease inflammation, improving liver disease [45]. Besides, uric acid, urea, and ornithine, an amino acid that plays a role in the urea cycle, increased after SVR. The increase of these metabolites is in line with previous studies, in which elevated serum uric acid was observed as an adverse effect of DAA therapy [46]. Increased alpha-ketoglutaric acid levels in the blood have been reported in liver diseases [47], so the reduced levels found in our study after DAA therapy could be linked to cirrhosis remission. However, it should be noted that the change in these metabolite levels could not be validated in the association analysis by GLMM. Thus, further investigation should be carried out to corroborate our findings.

Our study has several strengths and limitations. Firstly, only HIV/HCV-coinfected patients with advanced cirrhosis were included, which provided high homogeneity to the analysis. Secondly, the repeated measure design (each patient is its control) gave robustness to our findings. Thirdly, this study provides novel and valuable information, as no metabolomic analysis investigating changes after DAAs therapy and their association with liver disease scores and inflammation has been previously published. As a limitation, the sample size was small, reducing the statistical power to detect significant associations. Additionally, we analyzed the metabolic changes from baseline to 36 weeks after SVR; however, performing a metabolomic analysis after longer follow-up would be of great interest.

## 5. Conclusions

In summary, plasma metabolomic profile changed after HCV clearance with all oral-DAAs in HIV/HCV-coinfected with advanced HCV-related cirrhosis. The decrease in taurocholic acid and increases in LPC(20:4) and 2-keto-n-caproic acid/2-keto-isocaproic acid were linked to improvements in cirrhosis scores. Besides, plasma level changes in LPC (20:4) and taurocholic acid could alleviate the inflammatory state. Further work should be done to assess the long-term clinical implications of these changes (liver decompensation, hepatocellular carcinoma, and death) and the potential utility of metabolomic profile for the non-invasive surveillance of cirrhotic patients at risk.

## Ethics approval and consent to participate

This study was approved by the Research Ethics Committee of the Institute of Health Carlos III (CEI42_2020/CEI41_2014) and was carried out according to the Declaration of Helsinki.

## Consent for publication

Not applicable.

## Availability of data and materials

The datasets used and analyzed during the current study may be made available by the corresponding author upon reasoned request.

## Funding

This study was supported by grants from Instituto de Salud Carlos III (ISCIII; grant numbers CP17CIII/00007 (MPY407/18) and PI18CIII/00028 (MPY385/18) to MAJS, PI14/01094, PI17/00657, and PI20/00474 to JB, PI14/01581, PI17/00903 and PI20/00507 to JGG, and PI14CIII/00011, PI17CIII/00003, and PI20CIII/00004 to SR) and Ministerio de Sanidad, Servicios Sociales e Igualdad (grant number EC11–241). The study was also funded by the Spanish AIDS Research Network (RD16/0025/0017, RD16/0025/0018 and RD16CIII/0002/0002) and Centro de Investigación Biomédica en Red (CIBER) en Enfermedades Infecciosas (CB21/13/00044 and CB21/13/00039). MAJS is a Miguel Servet researcher supported and funded by ISCIII (grant number: CP17CIII/00007). JB is an investigator from the Programa de Intensificación de la Actividad Investigadora en el Sistema Nacional de Salud (I3SNS), Refs INT16/00100. CB and DR acknowledge funding from the Ministerio de Ciencia, Innovación y Universidades (RTI2018–095166-B-I00).

## CRediT authorship contribution statement

Funding body: MAJS and SR.

Study concept and design: MAJS.

Patients' selection and clinical data acquisition: JB, JGG, CD, VH, TAE, and RM.

Sample preparation, and biomarker analysis: AVB, DR, OBK, AFR, and CB.

Statistical analysis and interpretation of data: AVB, IM, and MAJS.

Writing of the manuscript: AVB and MAJS.

Critical revision of the manuscript for relevant intellectual content: IM and SR.

Supervision and visualization: MAJS and SR.

All authors approved the final version of the article.

## Conflict of interest statement

The authors declare that they have no competing interests.

## Data availability

Data will be made available on request.

## Acknowledgments

This study would not have been possible without the collaboration of all the patients, medical and nursery staff, and data managers who have taken part in the project. We want to particularly acknowledge the support of the HIV BioBank, which is integrated into the Spanish AIDS Research Network and all collaborating Centres, for the generous contribution with clinical samples for the present work (see **Appendix**). All authors approved the final version of the article, including the authorship list.

*Authors' information (optional)*

Not applicable.

## Appendix

**The ESCORIAL study group.**

**Hospital General Universitario Gregorio Marañón (**Madrid, Spain): Cristina Díez, Luis Ibáñez, Leire Pérez-Latorre, Diego Rincón, Teresa Aldámiz-Echevarría, Vega Catalina, Pilar Miralles, Teresa Aldámiz-Echevarría, Francisco Tejerina, María C Gómez-Rico, Esther Alonso, José M Bellón, Rafael Bañares, and Juan Berenguer.

**Hospital Universitario La Paz/IdiPAZ (**Madrid, Spain): José Arribas, José I Bernardino, Carmen Busca, Ana Delgado, Javier García-Samaniego, Víctor Hontañón, Luz Martín-Carbonero, Rafael Micán, María L Montes-Ramírez, Victoria Moreno, Antonio Olveira, Ignacio Pérez-Valero, Eulalia valencia, and Juan González-García.

**Hospital Universitario Puerta de Hierro** (Madrid, Spain): Elba Llop and José Luis Calleja.

**Hospital Universitario Ramón y Cajal** (Madrid, Spain): Javier Martínez and Agustín Albillos.

**Fundación SEIMC/GeSIDA** (Madrid, Spain): Marta de Miguel, María Yllescas, and Herminia Esteban.

## Appendix A. Supporting information

Supplementary data associated with this article can be found in the online version at doi:10.1016/j.biopha.2022.112623.

## References


[1] R.H. Westbrook, G. Dusheiko, Natural history of hepatitis C, J. Hepatol. 61 (1 Suppl) (2014) S58–S68.

[2] J. Macias, J. Berenguer, M.A. Japon, J.A. Giron, A. Rivero, L.F. Lopez-Cortes, A. Moreno, M. Gonzalez-Serrano, J.A. Iribarren, E. Ortega, P. Miralles, J.A. Mira, J. A. Pineda, Fast fibrosis progression between repeated liver biopsies in patients coinfected with human immunodeficiency virus/hepatitis C virus, Hepatology 50 (4) (2009) 1056–1063.

[3] A.H. Mohsen, P.J. Easterbrook, C. Taylor, B. Portmann, R. Kulasegaram, S. Murad, M. Wiselka, S. Norris, Impact of human immunodeficiency virus (HIV) infection on the progression of liver fibrosis in hepatitis C virus infected patients, Gut 52 (7) (2003) 1035–1040.

[4] P. Pradat, V. Virlogeux, E. Trepo, Epidemiology and elimination of HCV-related liver disease, Viruses 10 (10) (2018).

[5] S. Ekpanyapong, K.R. Reddy, Hepatitis C virus therapy in advanced liver disease: outcomes and challenges, United European, Gastroenterol. J. 7 (5) (2019) 642–650.

[6] S. Resino, M. Sanchez-Conde, J. Berenguer, Coinfection by human immunodeficiency virus and hepatitis C virus: noninvasive assessment and staging of fibrosis, Curr. Opin. Infect. Dis. 25 (5) (2012) 564–569.

[7] Y. Peng, X. Qi, X. Guo, Child-pugh versus MELD score for the assessment of prognosis in liver cirrhosis: a systematic review and meta-analysis of observational studies, Med. (Baltim. ) 95 (8) (2016), e2877.

[8] R. Paternostro, T. Reiberger, T. Bucsics, Elastography-based screening for esophageal varices in patients with advanced chronic liver disease, World J. Gastroenterol. 25 (3) (2019) 308–329.

[9] F.F. Fernandes, J. Piedade, L. Guimaraes, E.P. Nunes, U. Chaves, R.V. Goldenzon, S. W. Cardoso, J. Duarte, B. Grinsztejn, V.G. Veloso, G. Pereira, H. Perazzo, Effectiveness of direct-acting agents for hepatitis C and liver stiffness changing after sustained virological response, J. Gastroenterol. Hepatol. 34 (2019) 2187–2195.

[10] J. Macias, R. Granados, F. Tellez, D. Merino, M. Perez, L.E. Morano, R. Palacios, M. Paniagua, M. Frias, N. Merchante, J.A. Pineda, R.I.S.H.E.Psg Hepavir Gehep, , Similar recovery of liver function after response to all-oral HCV therapy in patients with cirrhosis with and without HIV coinfection, J. Viral Hepat. 26 (1) (2019) 16–24.

[11] Y.C. Lee, T.H. Hu, C.H. Hung, S.N. Lu, C.H. Chen, J.H. Wang, The change in liver stiffness, controlled attenuation parameter and fibrosis-4 index for chronic hepatitis C patients with direct-acting antivirals, PLoS One 14 (4) (2019), e0214323.

[12] N. Afdhal, G.T. Everson, J.L. Calleja, G.W. McCaughan, J. Bosch, D.M. Brainard, J. G. McHutchison, S. De-Oertel, D. An, M. Charlton, K.R. Reddy, T. Asselah, E. Gane, M.P. Curry, X. Forns, Effect of viral suppression on hepatic venous pressure gradient in hepatitis C with cirrhosis and portal hypertension, J. Viral Hepat. 24 (10) (2017) 823–831.

[13] S. Lens, E. Alvarado-Tapias, Z. Marino, M.C. Londono, L.L.E. Martinez J., J. I. Fortea, L. Ibanez, X. Ariza, A. Baiges, A. Gallego, R. Banares, A. Puente, A. Albillos, J.L. Calleja, X. Torras, V. Hernandez-Gea, J. Bosch, C. Villanueva, X. Forns, J.C. Garcia-Pagan, Effects of all-oral anti-viral therapy on HVPG and systemic hemodynamics in patients with hepatitis C virus-associated cirrhosis, Gastroenterology 153 (5) (2017) 1273–1283, e1.

[14] M. Mandorfer, K. Kozbial, P. Schwabl, C. Freissmuth, R. Schwarzer, R. Stern, D. Chromy, A.F. Stattermayer, T. Reiberger, S. Beinhardt, W. Sieghart, M. Trauner, H. Hofer, A. Ferlitsch, P. Ferenci, M. Peck-Radosavljevic, Sustained virologic response to interferon-free therapies ameliorates HCV-induced portal hypertension, J. Hepatol. 65 (4) (2016) 692–699.

[15] I. Gentile, R. Scotto, C. Coppola, L. Staiano, D.C. Amoruso, T. De Simone, F. Portunato, S. De Pascalis, S. Martini, M. Macera, G. Viceconte, G. Tosone, A. R. Buonomo, G. Borgia, N. Coppola, Treatment with direct-acting antivirals improves the clinical outcome in patients with HCV-related decompensated cirrhosis: results from an Italian real-life cohort (Liver Network Activity-LINA cohort), Hepatol. Int. 13 (1) (2019) 66–74.

[16] O. El-Sherif, Z.G. Jiang, E.B. Tapper, K.C. Huang, A. Zhong, A. Osinusi, M. Charlton, M. Manns, N.H. Afdhal, K. Mukamal, J. McHutchison, D.M. Brainard, N. Terrault, M.P. Curry, Baseline factors associated with improvements in decompensated cirrhosis after direct-acting antiviral therapy for hepatitis C virus infection, Gastroenterology 154 (8) (2018) 2111–2121, e8.

[17] G.W. McCaughan, P.A. Thwaites, S.K. Roberts, S.I. Strasser, J. Mitchell, B. Morales, S. Mason, P. Gow, A. Wigg, C. Tallis, G. Jeffrey, J. George, A.J. Thompson, F. C. Parker, P.W. Angus, N. Australian, Liver association clinical research, sofosbuvir and daclatasvir therapy in patients with hepatitis C-related advanced decompensated liver disease (MELD >/= 15), Aliment Pharmacol. Ther. 47 (3) (2018) 401–411.

[18] L.M. Medrano, J. Berenguer, S. Salguero, J. Gonzalez-Garcia, C. Diez, V. Hontanon, P. Garcia-Broncano, L. Ibanez-Samaniego, J.M. Bellon, M.A. Jimenez-Sousa, S. Resino, Successful HCV therapy reduces liver disease severity and inflammation biomarkers in HIV/HCV-coinfected patients with advanced cirrhosis: a cohort study, Front. Med. (Lausanne) 8 (2021), 615342.

[19] D.L. Wyles, M.S. Sulkowski, D. Dieterich, Management of hepatitis C/HIV coinfection in the era of highly effective hepatitis C virus direct-acting antiviral therapy, Clin. Infect. Dis. 63 (Suppl 1) (2016) S3–S11.

[20] C. Diez, J. Berenguer, L. Ibanez-Samaniego, E. Llop, L. Perez-Latorre, M. V. Catalina, V. Hontanon, M.A. Jimenez-Sousa, T. Aldamiz-Echevarria, J. Martinez, J.L. Calleja, A. Albillos, J.M. Bellon, S. Resino, J. Gonzalez-Garcia, R. Banares, Persistence of clinically significant portal hypertension after eradication of hepatitis C virus in patients with advanced cirrhosis, Clin. Infect. Dis. 71 (10) (2020) 2726–2729.

[21] S. Salguero, D. Rojo, J. Berenguer, J. Gonzalez-Garcia, A. Fernandez-Rodriguez, O. Brochado-Kith, C. Diez, V. Hontanon, A. Virseda-Berdices, J. Martinez, L. Ibanez-Samaniego, E. Llop-Herrera, C. Barbas, S. Resino, M.A. Jimenez-Sousa, G. Escorial Study, Plasma metabolomic fingerprint of advanced cirrhosis stages among HIV/HCV-coinfected and HCV-monoinfected patients, Liver Int. 40 (9) (2020) 2215–2227.

[22] S. Naggie, S. Lusk, J.W. Thompson, M. Mock, C. Moylan, J.E. Lucas, L. Dubois, L. John-Williams St, M.A. Moseley, K. Patel, Metabolomic signature as a predictor of liver disease events in patients with HIV/HCV coinfection, J. Infect. Dis. 222 (12) (2020) 2012–2020.

[23] L.M. Medrano, P. Garcia-Broncano, J. Berenguer, J. Gonzalez-Garcia, M. A. Jimenez-Sousa, J.M. Guardiola, M. Crespo, C. Quereda, J. Sanz, I. Canorea, A. Carrero, V. Hontanon, M.A. Munoz-Fernandez, S. Resino, G.b.S. group, elevated liver stiffness is linked to increased biomarkers of inflammation and immune activation in HIV/hepatitis C virus-coinfected patients, AIDS 32 (9) (2018) 1095–1105.

[24] A. Binek, D. Rojo, J. Godzien, F.J. Ruperez, V. Nunez, I. Jorge, M. Ricote, J. Vazquez, C. Barbas, Flow cytometry has a significant impact on the cellular metabolome, J. Proteome Res 18 (1) (2019) 169–181.

[25] T. Kind, G. Wohlgemuth, D.Y. Lee, Y. Lu, M. Palazoglu, S. Shahbaz, O. Fiehn, FiehnLib: mass spectral and retention index libraries for metabolomics based on quadrupole and time-of-flight gas chromatography/mass spectrometry, Anal. Chem. 81 (24) (2009) 10038–10048.

[26] A. Gil-de-la-Fuente, J. Godzien, S. Saugar, R. Garcia-Carmona, H. Badran, D. S. Wishart, C. Barbas, A. Otero, CEU mass mediator 3.0: a metabolite annotation tool, J. Proteome Res 18 (2) (2019) 797–802.

[27] S.A. Sansone, T. Fan, R. Goodacre, J.L. Griffin, N.W. Hardy, R. Kaddurah-Daouk, B. S. Kristal, J. Lindon, P. Mendes, N. Morrison, B. Nikolau, D. Robertson, L. W. Sumner, C. Taylor, M. van der Werf, B. van Ommen, O. Fiehn, M.B. Members, The metabolomics standards initiative, Nat. Biotechnol. 25 (8) (2007) 846–848.

[28] R.M. Salek, C. Steinbeck, M.R. Viant, R. Goodacre, W.B. Dunn, The role of reporting standards for metabolite annotation and identification in metabolomic studies, Gigascience 2 (1) (2013) 13.

[29] G. Meoni, S. Lorini, M. Monti, F. Madia, G. Corti, C. Luchinat, A.L. Zignego, L. Tenori, L. Gragnani, The metabolic fingerprints of HCV and HBV infections studied by nuclear magnetic resonance spectroscopy, Sci. Rep. 9 (1) (2019) 4128.

[30] S. Heimerl, M. Fischer, A. Baessler, G. Liebisch, A. Sigruener, S. Wallner, G. Schmitz, Alterations of plasma lysophosphatidylcholine species in obesity and weight loss, PLoS One 9 (10) (2014), e111348.

[31] K. Diamanti, M. Cavalli, G. Pan, M.J. Pereira, C. Kumar, S. Skrtic, M. Grabherr, U. Riserus, J.W. Eriksson, J. Komorowski, C. Wadelius, Intra- and inter-individual metabolic profiling highlights carnitine and lysophosphatidylcholine pathways as key molecular defects in type 2 diabetes, Sci. Rep. 9 (1) (2019) 9653.

[32] E. Sidorov, D.K. Sanghera, J.K.P. Vanamala, Biomarker for ischemic stroke using metabolome: a clinician perspective, J. Stroke 21 (1) (2019) 31–41.

[33] A.D. Patterson, O. Maurhofer, D. Beyoglu, C. Lanz, K.W. Krausz, T. Pabst, F. J. Gonzalez, J.F. Dufour, J.R. Idle, Aberrant lipid metabolism in hepatocellular carcinoma revealed by plasma metabolomics and lipid profiling, Cancer Res 71 (21) (2011) 6590–6600.

[34] L.A. Taylor, J. Arends, A.K. Hodina, C. Unger, U. Massing, Plasma lyso-phosphatidylcholine concentration is decreased in cancer patients with weight loss and activated inflammatory status, Lipids Health Dis. 6 (2007) 17.

[35] V.N. Bochkov, O.V. Oskolkova, K.G. Birukov, A.L. Levonen, C.J. Binder, J. Stockl, Generation and biological activities of oxidized phospholipids, Antioxid. Redox Signal 12 (8) (2010) 1009–1059.

[36] S. Freigang, The regulation of inflammation by oxidized phospholipids, Eur. J. Immunol. 46 (8) (2016) 1818–1825.

[37] Y. Muto, S. Sato, A. Watanabe, H. Moriwaki, K. Suzuki, A. Kato, M. Kato, T. Nakamura, K. Higuchi, S. Nishiguchi, H. Kumada, L.-T.S.S. Group, Effects of oral branched-chain amino acid granules on event-free survival in patients with liver cirrhosis, Clin. Gastroenterol. Hepatol. 3 (7) (2005) 705–713.

[38] S. Hayaishi, H. Chung, M. Kudo, E. Ishikawa, M. Takita, T. Ueda, S. Kitai, T. Inoue, N. Yada, S. Hagiwara, Y. Minami, K. Ueshima, Oral branched-chain amino acid granules reduce the incidence of hepatocellular carcinoma and improve event-free survival in patients with liver cirrhosis, Dig. Dis. 29 (3) (2011) 326–332.

[39] M. Moghei, P. Tavajohi-Fini, B. Beatty, O.A. Adegoke, Ketoisocaproic acid, a metabolite of leucine, suppresses insulin-stimulated glucose transport in skeletal muscle cells in a BCAT2-dependent manner, Am. J. Physiol. Cell Physiol. 311 (3) (2016) C518–C527.

[40] U.M. Kujala, M. Peltonen, M.K. Laine, J. Kaprio, O.J. Heinonen, J. Sundvall, J. G. Eriksson, A. Jula, S. Sarna, H. Kainulainen, Branched-chain amino acid levels are related with surrogates of disturbed lipid metabolism among older men, Front Med (Lausanne) 3 (2016) 57.

[41] A. Do, D.A. Esserman, S. Krishnan, J.K. Lim, T.H. Taddei, R.G. Hauser, 3rd, J. P. Tate, V.L. Re, 3rd, A.C. Justice, Excess weight gain after cure of hepatitis c infection with direct-acting antivirals, J. Gen. Intern Med 35 (7) (2020) 2025–2034.

[42] J.S. Bajaj, S. Fan, L.R. Thacker, A. Fagan, E. Gavis, M.B. White, D.M. Heuman, M. Fuchs, O. Fiehn, Serum and urinary metabolomics and outcomes in cirrhosis, PLoS One 14 (9) (2019), e0223061.
[43] M. Nguyen, A. Sharma, W. Wu, R. Gomi, B. Sung, D. Hospodsky, L.T. Angenent, S. Worgall, The fermentation product 2,3-butanediol alters P. aeruginosa clearance, cytokine response and the lung microbiome, ISME J. 10 (12) (2016) 2978–2983.
[44] Z. Liu, Z. Zhang, M. Huang, X. Sun, B. Liu, Q. Guo, Q. Chang, Z. Duan, Taurocholic acid is an active promoting factor, not just a biomarker of progression of liver cirrhosis: evidence from a human metabolomic study and in vitro experiments, BMC Gastroenterol. 18 (1) (2018) 112.
[45] D.Y. Lee, E.H. Kim, Therapeutic effects of amino acids in liver diseases: current studies and future perspectives, J. Cancer Prev. 24 (2) (2019) 72–78.
[46] K. Sato, A. Naganuma, T. Nagashima, T. Hoshino, D. Uehara, Y. Arai, K. Horiuchi, K. Yuasa, H. Takayama, H. Arai, T. Hatanaka, T. Ohyama, H. Tahara, N. Sohara, T. Kobayashi, N. Horiguchi, Y. Yamazaki, S. Kakizaki, M. Kusano, M. Yamada, T. Murase, T. Nakamura, Elevated serum uric acid level was a notable adverse event during combination therapy with sofosbuvir and ribavirin, Hepatol. Res 48 (3) (2018) E347–E353.
[47] A.M. Dawson, J. De Groote, W.S. Rosenthal, S. Sherlock, Blood pyruvic-acid and alpha-ketoglutaric-acid levels in liver disease and hepatic coma, Lancet 272 (6965) (1957) 392–396.